Journal of Catalysis 258 (2008) 5–13

Contents lists available at ScienceDirect

Journal of Catalysis

www.elsevier.com/locate/jcat

Fe-containing ionic liquids as catalysts for the dimerization of bicyclo[2.2.1]hepta-2,5-diene

Mai Dao Nguyen, Ly Vinh Nguyen, Eun Hee Jeon, Jin Hyung Kim, Minserk Cheong, Hoon Sik Kim *, Je Seung Lee *

Department of Chemistry and Research Institute of Basic Sciences, Kyung Hee University, 1 Hoegi-dong, Dongdaemoon-gu, Seoul 130-701, Republic of Korea

ARTICLE INFO

Article history:
Received 21 January 2008
Revised 27 March 2008
Accepted 11 May 2008
Available online 11 July 2008

Keywords:
Ionic liquids
$FeCl_3$
$FeCl_2$
Diethylaluminum chloride
2,5-Norbornadiene
Dimerization
Hexacyclic endo–endo isomer

ABSTRACT

Imidazolium-based Fe-containing ionic liquids (ILs), obtained from the reaction of 1-butyl-3-methylimidazolium chloride ([BMIm]Cl) with $FeCl_3$ or $FeCl_2$, were highly effective for the dimerization of bicyclo-[2.2.1]hepta-2,5-diene (2,5-norbornadiene, NBD) in the presence of diethylaluminum chloride (DEAC). Fe-containing ILs produced hexacyclic endo–endo NBD dimer (H_{nn}) in high yield and selectivity, whereas $FeCl_3$ yielded large amounts of side products. The yield and selectivity of H_{nn} were affected by the degree of reduction of Fe(III) compounds by DEAC to Fe(II) species as determined by X-ray photoelectron spectroscopy. Higher yield of H_{nn} was obtained with the catalytic system producing larger amounts of Fe(II) species. Theoretical calculation and experimental results support that Fe(II) is the active species for the dimerization.

1. Introduction

Bicyclo[2.2.1]hepta-2,5-diene (2,5-norbornadiene, NBD) dimers, ingredients of high density liquid fuels (HDLF) and lubricants, have been prepared from the cyclodimerization of NBD in the presence of a catalyst or a catalytic system mostly based on transition metal, such as cobalt [1–3], iron [4–7], nickel [8–11], and rhodium [12–15]. In many cases, however, the dimerization produces a wide range of isomeric mixtures as shown in Scheme 1, depending on the type of catalyst employed. For instance, Rh/C catalyst favors the formation of hexacyclic exo-endo (H_{xn}) as the major product [12]. The use of three-component catalytic system consisting of Co(acetylacetonate)$_3$ (Co(acac)$_3$), triphenylphosphine (TPP), and diethylaluminum chloride (DEAC) or ethylaluminum dichloride (EADC) produces heptacyclic Binor-S (dodecahydro-1,2,4:5,6,8-dimetheno-s-indecene) as the major product [1]. In contrast, the dimerization in the presence of an iron-based three-component catalytic system (Fe(acac)$_3$, TPP, and DEAC or EADC) yields hexacyclic endo–endo dimer (hexacyclo[7.2.1.$0^{2,8}$.$1^{3,7}$.$1^{5,13}$.$0^{4,6}$]tetradec-10-ene, H_{nn}) as the major product [5].

In general, the dimerization of NBD to obtain H_{nn} as the major product requires the use of additives such as alkylaluminum chloride and trialkyl or triarylphosphanes (PR_3) [1,5–7,12]. Alkylaluminum chlorides are known to reduce metal complexes to form active species and PR_3 are believed to function as stabilizers for the resulting active species [16]. Therefore, to obtain H_{nn} in high yields and selectivities, a suitable combination of metal complex and additives is of pivotal importance. One major problem associated with the current catalytic systems for the synthesis of H_{nn} is the use of expensive Fe(acac)$_3$ and PR_3 as the key components.

Recently, there has been a considerable interest in the application of ionic liquids (ILs) to the immobilization of volatile, precious, and/or toxic homogeneous catalysts to improve the stability and recovery of the catalysts [17].

In the continuous line of our work on the development of active, selective, and cost effective catalytic systems for the dimerization of NBD, we have found that the Fe-based ILs are highly active and selective for the production of H_{nn} without use of expensive Fe(acac)$_3$ and PR_3.

Herein, we report an active catalytic system consisting of a Fe-containing IL and DEAC for the selective production of H_{nn} from the dimerization of NBD.

2. Experimental

2.1. Chemicals

NBD, DEAC, $FeCl_3$, and $FeCl_2$ were purchased from Aldrich Chemical Co. and used without further purification. All of the solvents were obtained from J.T. Baker Chemical Co. and were distilled over appropriate drying agents prior to use [18]. 1-Butyl-3-methylimidazolium chloride ([BMIm]Cl), [BMIm]$_2$FeCl$_4$, and

* Corresponding authors. Fax: +82 2 965 4408.
E-mail addresses: khs2004@khu.ac.kr (H.S. Kim), leejs70@khu.ac.kr (J.S. Lee).

0021-9517/$ – see front matter
doi:10.1016/j.jcat.2008.05.008

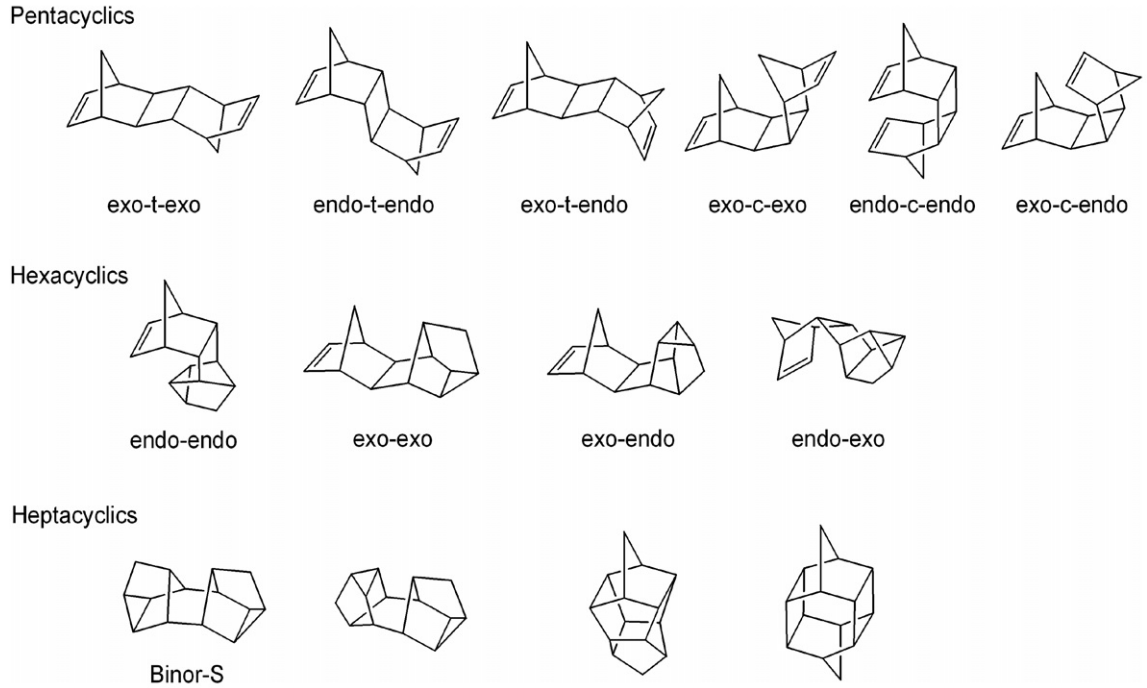

Scheme 1. Theoretically possible dimers of NBD.

$[BMIm]Fe_xCl_{3x+1}$ ($x = 1$ or 2) were prepared using the methods described in the literature [19–21].

2.2. Synthesis of Fe-containing ILs

The reaction of [BMIm]Cl (3.49 g, 20 mmol) with $FeCl_3$ (3.24 g, 20 mmol) at a room temperature for 3 h produced $[BMIm]FeCl_4$ as a pale yellow liquid. Negative-ions ESI-MS spectra: m/z 197.63 $[FeCl_4]^-$, 100%; m/z 534.61 $([BMIm][FeCl_4]_2)^-$, 15%.

$[BMIm]Fe_2Cl_7$ was prepared in a manner analogous to that employed for the synthesis of $[BMIm]FeCl_4$ by reacting [BMIm]Cl with two equivalents of $FeCl_3$. Negative-ions ESI-MS spectra: m/z 197.63 $[FeCl_4]^-$, 100%; m/z 358.46 $[Fe_2Cl_7]^-$, 39%.

2.3. Instruments

The products were analyzed by gas chromatography with an Agilent 6890 GC equipped with a flame ionized detector and a DB wax column (30 m × 0.32 mm × 0.25 μm) and by mass spectrometry with an Agilent 6890-5975 GC-MSD equipped with a HP-5 capillary column (50 m × 0.2 mm × 0.5 μm). The one-electron reduction potentials of iron-containing ILs were obtained by means of Tafel measurement (PARSTAT 2263, Princeton Applied Research) at an ambient temperature. A platinum working electrode of 1.2 mm diameter was used with a platinum wire as the counter electrode and a silver wire as a quasi reference electrode. The experimental solution (0.1 M tetrabutylammonium perchlorate in dichloromethane) was deaerated prior to measurement. The polarization scan was from −250 mV vs E_{OC} (open circuit potential) to +250 mV vs E_{OC} at a rate of 10 mV s^{-1}.

X-ray photoelectron spectroscopy (XPS) measurements were conducted with a PHI 5800 ESCA System of Physical Electronics equipped with a hemispherical energy analyzer and the monochromatized Al$K\alpha$ X-ray source of 250 W. The pass energy was 93.9 eV (0.8 eV steps) and 58.7 eV (0.13 eV steps) for the survey and high-resolution spectra, respectively. The collection angle for all the measurements was 45°. Before data acquisition, the catalyst sample was degassed for 3 h at 298 K under a reduced pressure of about 1.0×10^{-9} Torr to minimize the surface contamination. Each spectrum obtained was curve-deconvoluted using the XPS-PEAK Version 4.1 software [22]. The C 1s peak at 284.6 eV was used to correct the surface charging effect before attempting the chemical state identification [23,24].

2.4. Dimerization reaction

Dimerization reactions of NBD were conducted in a 100 mL 3-neck round bottomed flask fitted with a reflux condenser, a thermocouple well, and a dropping funnel under a nitrogen atmosphere. The flask was charged with a catalyst, DEAC, toluene as a solvent, and *m*-xylene as an internal standard. The flask was then immersed in an oil bath that was maintained at a specified temperature. NBD was added slowly through the dropping funnel at the reaction temperature. After neutralization of the product mixture with an aqueous solution of $NaHCO_3$, the organic layer was recovered and analyzed by GC, GC-Mass, and ^{1}H NMR [25].

3. Results and discussion

3.1. Effects of DEAC and [BMIm]Cl

The effects of DEAC and [BMIm]Cl on the $FeCl_3$-catalyzed dimerization of NBD were investigated at 85 °C and at the molar ratio of NBD/catalyst of 50. Table 1 shows that either $FeCl_3$ or DEAC was inactive for the dimerization when used alone. However, the combined use of $FeCl_3$ and DEAC resulted in almost quantitative conversion of NBD along with the formation of large quantities of high boiling side products (entry 3). Even though the selectivity of H_{nn} was as low as 13.6%, this result clearly demonstrated the important role of DEAC in the activation of $FeCl_3$. Interestingly, the selectivity and yield of H_{nn} increased significantly when [BMIm]Cl was added to the catalytic system consisting of $FeCl_3$ and DEAC (entry 6). Since the role of alkylaluminum chloride is to reduce and/or to activate metal complexes, the activity of Fe(III)-based catalytic system and the product composition will obviously be affected by the degree of reduction of Fe(III) compound by DEAC and

Table 1
Activities of various catalytic systems for the dimerization of NBD[a,b]

Entry	Catalyst	C[b] (%)	S[c] (%)	Y[d] (%)
1	DEAC	0.0	0.0	0.0
2	$FeCl_3$	0.0	0.0	0.0
3	$FeCl_3$–DEAC (1:5)	98.8	13.6	13.4
4	$FeCl_3$–[BMIm]Cl (1:1)	0.0	0.0	0.0
5	[BMIm]$FeCl_4$–DEAC (1:5)	78.1	74.1	57.9
6	$FeCl_3$–[BMIm]Cl–DEAC (1:1:5)[e]	73.8	73.9	54.5

[a] Molar ratio of NBD/Fe(III) = 50, temperature = 85 °C, reaction time = 1 h. Numbers in parentheses refer to molar ratios.
[b] Conversion of NBD.
[c] Selectivity of H_{nn}.
[d] Yield of H_{nn}.
[e] $FeCl_3$ and [BMIm]Cl were added separately.

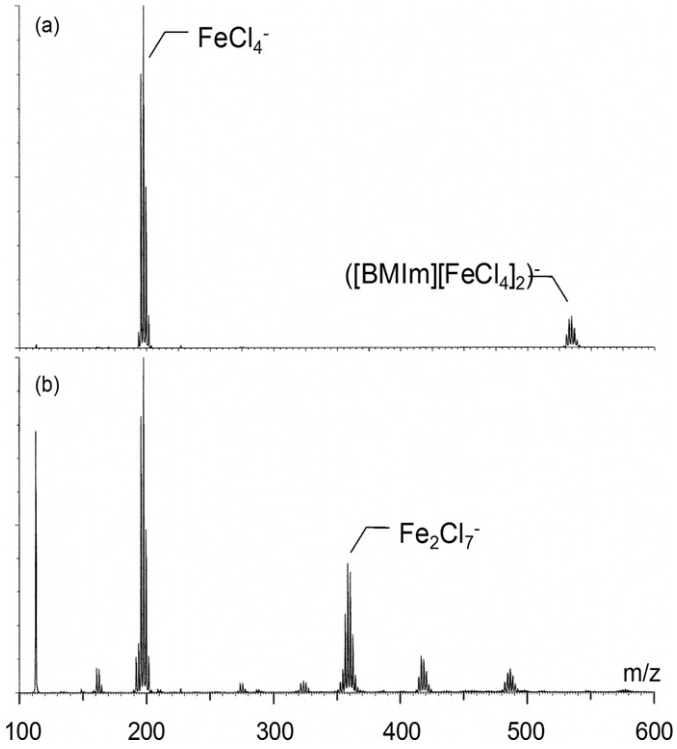

Fig. 1. Negative ions ESI-MS spectra of (a) [BMIm]$FeCl_4$ and (b) [BMIm]Fe_2Cl_7.

also by the nature of the reduced Fe species. $FeCl_3$ is well known to react with an equimolar amount of [BMIm]Cl to form an IL, [BMIm]$FeCl_4$ [20,21]. Therefore, the higher H_{nn} selectivity with the catalytic system consisting of $FeCl_3$, [BMIm]Cl, and DEAC can be largely attributed to the in situ formation of [BMIm]$FeCl_4$. Following reduction by DEAC is likely to generate an active Fe species for the dimerization of NBD. In fact, the catalytic system composed of [BMIm]$FeCl_4$ and DEAC gave similar H_{nn} yield to that consisting of $FeCl_3$, [BMIm]Cl, and DEAC, suggesting that [BMIm]$FeCl_4$ is formed in situ from $FeCl_3$ and [BMIm]Cl (entry 5).

3.2. Activities of Fe-containing ILs

Fe-containing imidazolium-based ILs were prepared from the reaction of $FeCl_3$ with [BMIm]Cl at different molar ratios of $FeCl_3$/[BMIm]Cl and used for the dimerization of NBD instead of using catalytic systems composed of $FeCl_3$ and [BMIm]Cl. As seen in Fig. 1, ESI-MS spectra of the Fe-containing ILs show that the mononuclear $[FeCl_4]^-$ was the major anionic Fe(III) species at the molar ratio of $FeCl_3$/[BMIm]Cl of 1. However, at the molar ratio of 2, the formation of high nuclear Fe(III) species, $[Fe_2Cl_7]^-$, was

Table 2
Effect of molar ratio of DEAC/catalyst[a]

Entry	Catalyst	Molar ratio (DEAC/catalyst)	C[b] (%)	S[c] (%)	Y[d] (%)
1	[BMIm]$FeCl_4$	–	0.0	0.0	0.0
2	[BMIm]$FeCl_4$	1	12.2	79.7	9.7
3	[BMIm]$FeCl_4$	2	50.9	80.2	40.8
4	[BMIm]$FeCl_4$	5	78.1	74.1	57.9
5	[BMIm]$FeCl_4$	10	97.6	78.2	76.3
6	[BMIm]Fe_2Cl_7	–	0.0	0.0	0.0
7	[BMIm]Fe_2Cl_7	1	30.0	84.5	25.4
8	[BMIm]Fe_2Cl_7	2	90.7	87.5	79.4
9	[BMIm]Fe_2Cl_7	5	96.9	76.4	74.0
10[e]	[BMIm]Fe_2Cl_7	5	96.0	77.8	74.7
11	[BMIm]Fe_2Cl_7	10	97.6	77.4	75.5

[a] Molar ratio of NBD/Fe(III) = 50, temperature = 85 °C, reaction time = 1 h.
[b] Conversion of NBD.
[c] Selectivity of H_{nn}.
[d] Yield of H_{nn}.
[e] Eight equivalents of TPP to Fe(III) was added.

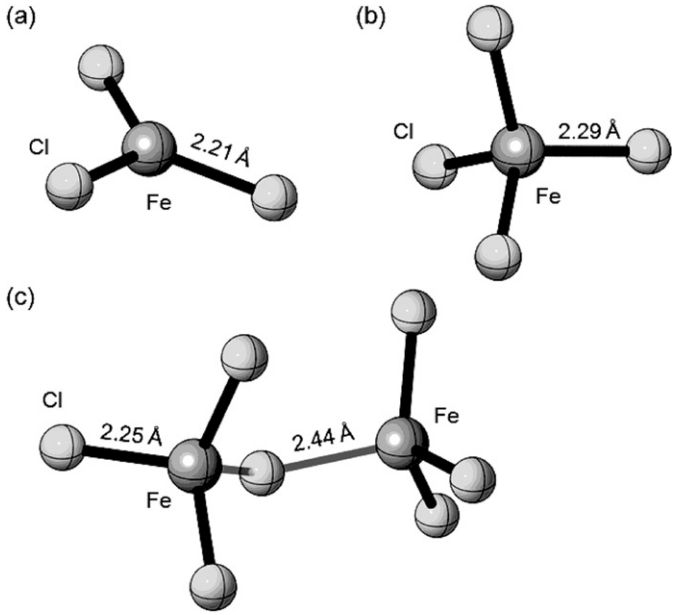

Fig. 2. Optimized structures of (a) $FeCl_3$, (b) $[FeCl_4]^-$, and (c) $[Fe_2Cl_7]^-$.

pronounced. It is reported that the reaction of $AlCl_3$ with [BMIm]Cl produces [BMIm]$AlCl_4$ and [BMIm]Al_2Cl_7 at the $AlCl_3$/[BMIm]Cl molar ratios of 1 and 2, respectively [26–28]. Likewise, the formation of [BMIm]Fe_2Cl_7 from the reaction of [BMIm]Cl with two equivalents of $FeCl_3$ can be easily conceivable [20].

Table 2 shows the dimerization activities of the Fe-containing ILs, [BMIm]$FeCl_4$ and [BMIm]Fe_2Cl_7. When the dimerization was carried out using [BMIm]$FeCl_4$ at 85 °C and at the molar ratio of NBD/Fe(III) = 50 for 1 h, the conversion of NBD and the yield of H_{nn} increased with increasing molar ratio of DEAC/[BMIm]$FeCl_4$. Interestingly, under the same experimental condition, [BMIm]-Fe_2Cl_7 produced much higher yield of H_{nn} in comparison with [BMIm]$FeCl_4$ up to the molar ratio of DEAC/Fe(III) = 5. These results could be attributed to the structural difference between [BMIm]$FeCl_4$ and [BMIm]Fe_2Cl_7 toward the reduction by DEAC.

To have a better insight on the activity difference between [BMIm]$FeCl_4$ and [BMIm]Fe_2Cl_7, the optimized structures of $FeCl_3$, $[FeCl_4]^-$, and $[Fe_2Cl_7]^-$ were calculated at the B3LYP (6-31+G* for C and H, and LanL2DZ with ECP for Cl and Fe) level of the theory using Gaussian 03 program, were compared [20]. A comparison of the Fe–Cl bond lengths in Fig. 2 shows that $[FeCl_4]^-$ has longer Fe–Cl bond distance than $FeCl_3$ by 0.08 Å. $[Fe_2Cl_7]^-$ has a

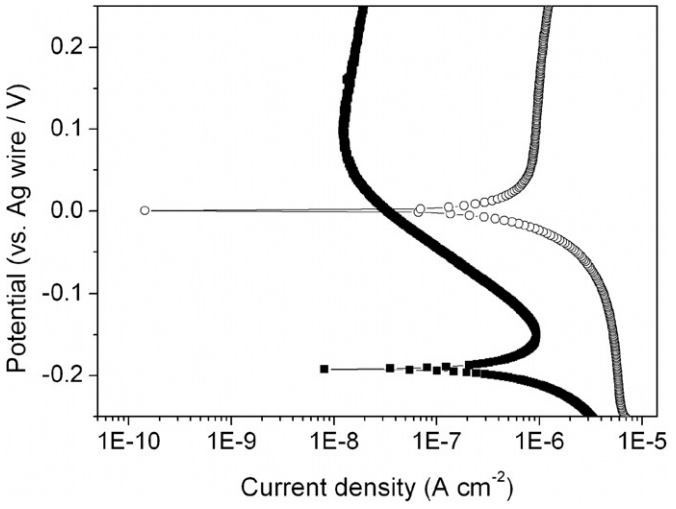

Fig. 3. Tafel plots of $[BMIm]Fe_2Cl_7$ (○) and $[BMIm]FeCl_4$ (■) at room temperature under N_2(g). A platinum working electrode of 1.2 mm diameter was used with a platinum wire as the counter electrode and a silver wire as a quasi reference electrode. The experimental solution (0.1 M tetrabutylammonium perchlorate in dichloromethane) was deaerated prior to measurement. The polarization scan was from −250 mV vs E_{OC} (open circuit potential) to +250 mV vs E_{OC} at a rate of 10 mV s^{-1}.

bridging and six terminal Cl atoms. The bond distance between Fe and the bridging Cl is 2.44 Å, which is longer by 0.15 Å than that in $[FeCl_4]^-$. From the structural analysis of Fe(III) compounds and the experimental results on the NBD dimerization, it is likely that the role of [BMIm]Cl is to facilitate the reduction of $FeCl_3$ by lengthening Fe–Cl bond through the formation of $[FeCl_4]^-$ and $[Fe_2Cl_7]^-$, and to stabilize the resulting active species.

The reduction of Fe-containing ILs by DEAC was supported by the Tafel measurement (see Fig. 3). The one-electron reduction potentials of $[FeCl_4]^-$ and $[Fe_2Cl_7]^-$ were observed at −0.192 and 0.001 V, respectively. This is a strong indication that Fe(III) is reduced to Fe(II) and the reduction of $[Fe_2Cl_7]^-$ is easier than $[FeCl_4]^-$. In this context, the higher catalytic performance of $[BMIm]Fe_2Cl_7$ can be ascribed to the easier reduction by DEAC arising from the presence of a loosely bound bridging chloride ligand in $[Fe_2Cl_7]^-$, thereby resulting in the generation of larger amounts of active Fe species.

The investigation of the effect of DEAC/Fe(III) molar ratio on the NBD dimerization strongly implies that the reduction of $[BMIm]Fe_2Cl_7$ by DEAC is easier than that of $[BMIm]FeCl_4$. As listed in Table 2, the NBD conversions and H_{nn} yields increased with increasing molar ratio of DEAC/Fe(III) for both $[BMIm]FeCl_4$ and $[BMIm]Fe_2Cl_7$, but the amount of DEAC required to achieve similar yield of H_{nn} was much less for $[BMIm]Fe_2Cl_7$ than that for $[BMIm]FeCl_4$.

The easier reduction of $[BMIm]Fe_2Cl_7$ by DEAC was further confirmed from the analysis of gas evolution during the reduction process. The amount of *n*-butane and ethyl chloride measured by GC and GC-Mass was much larger for $[BMIm]Fe_2Cl_7$ than for $[BMIm]FeCl_4$.

3.3. Mechanistic investigation

To elucidate the nature of active species and to have a better understanding of the role of [BMIm]Cl and DEAC, the high-resolution XPS analysis of the catalytic systems was conducted. The Fe $2p_{3/2}$ and Cl 2p peaks were deconvoluted using XPSPEAK Version 4.1 software using a Gaussian–Lorentzian peak profile function and a Shirley background [22]. It is reported that the characteristic Fe $2p_{3/2}$ peaks for Fe(III), Fe(II), and Fe(0) appeared

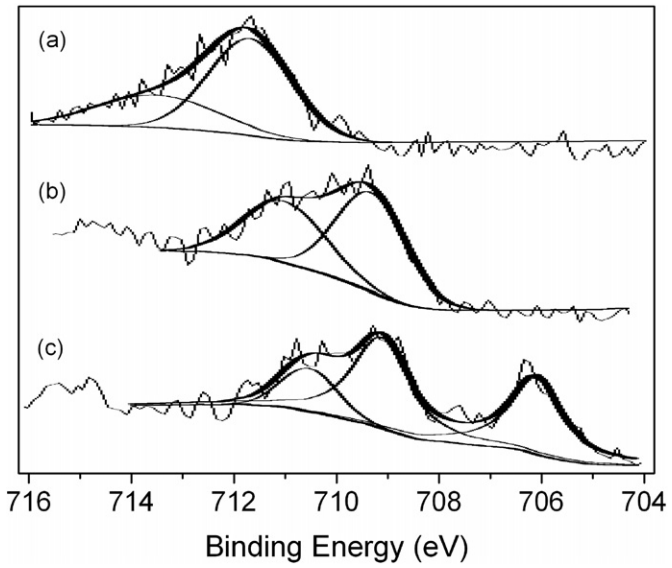

Fig. 4. Curve-fitted XPS high-resolution Fe $2p_{3/2}$ spectra of (a) $[BMIm]Fe_2Cl_7$, (b) $[BMIm]FeCl_4$ with DEAC, and (c) $[BMIm]Fe_2Cl_7$ with DEAC.

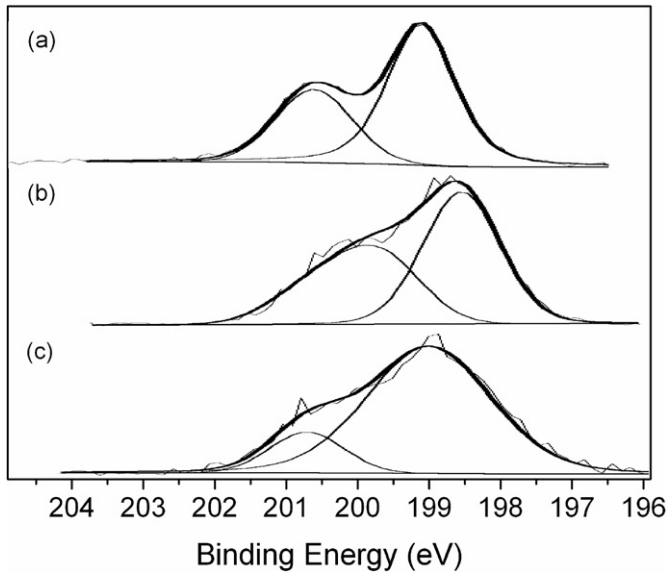

Fig. 5. Curve-fitted XPS high-resolution Cl 2p spectrum of (a) $[BMIm]Fe_2Cl_7$, (b) $[BMIm]FeCl_4$ with DEAC, and (c) $[BMIm]Fe_2Cl_7$ with DEAC.

at 711.2, 709.8, and 706.7 eV, respectively [22,23,29]. As shown in Fig. 4, $[BMIm]Fe_2Cl_7$ exhibited two distinct peaks of Fe $2p_{3/2}$ at 713.6 and 711.8 eV corresponding to Fe(III) with the area ratio of 1:1.7, implying that two different coordination environments exist for Fe(III). When $[BMIm]Fe_2Cl_7$ was treated with DEAC at 85 °C, the high-resolution spectrum of Fe $2p_{3/2}$ showed three component peaks at 710.5, 709.1, and 706.0 eV associated with Fe(III), Fe(II), and Fe(0), respectively. The area ratio of Fe(III)/Fe(II)/Fe(0) was calculated as 1/3.2/2.4, indicating that about 85% of Fe(III) was reduced to Fe(II) and Fe(0). In contrast, the reduction of $[BMIm]FeCl_4$ by DEAC showed two component peaks at 711.1 and 709.3 eV corresponding to Fe(III) and Fe(II) with the area ratio of Fe(III)/Fe(II) = 1/1.3, clearly demonstrating that $[BMIm]Fe_2Cl_7$ can be more easily reduced by DEAC than $[BMIm]FeCl_4$.

Further information on the chemical structure of the active species was obtained from a close analysis of the Cl 2p spectrum. As seen in Fig. 5, the chloride ions in $[BMIm]Fe_2Cl_7$ were in two different energy states, evidenced by the two peaks at 200.7

Table 3
Activities of catalytic systems based on Fe(0) and $FeCl_2$ for the dimerization of NBD[a]

Entry	Catalyst	C[b] (%)	S[c] (%)	Y[d] (%)
1[e]	Fe(0)	0.0	0.0	0.0
2[e]	Fe(0)–[BMIm]Cl (1:1)	0.0	0.0	0.0
3[e]	Fe(0)–TPP (1:5)	0.0	0.0	0.0
4[e]	Fe(0)–[BMIm]Cl–DEAC (1:1:5)	0.0	0.0	0.0
5[e]	Fe(0)–[BMIm]Cl–TPP–DEAC (1:1:3:5)	0.0	0.0	0.0
6	$FeCl_2$	0.0	0.0	0.0
7	$FeCl_2$–[BMIm]Cl (1:1)	0.0	0.0	0.0
8	$FeCl_2$–DEAC (1:5)	0.0	0.0	0.0
9	$FeCl_2$–[BMIm]Cl–DEAC (1:0.5:2.5)	58.2	79.4	46.2
10	$FeCl_2$–[BMIm]Cl–DEAC (1:1:2.5)	80.1	73.8	59.1
11	$FeCl_2$–[BMIm]Cl–DEAC (1:2:5)	88.9	78.7	70.0
12	$FeCl_2$–[BMIm]Cl–DEAC (1:3:5)	91.2	77.5	70.7
13	$Fe(acac)_3$–TPP–DEAC (1:4:10)	85.3	83.0	70.8

[a] Molar ratio of NBD/Fe = 50, temperature = 85 °C, reaction time = 1 h. Numbers in parentheses refer to molar ratios.
[b] Conversion of NBD.
[c] Selectivity of H_{nn}.
[d] Yield of H_{nn}.
[e] Fe(0): Fe powder, Fe nanoparticles, or $Fe(CO)_5$.

and 199.2 eV. The presence of two peaks with the area ratio of 1:1.8 indicates that the charge is asymmetrically distributed on two Fe atoms of $Fe_2Cl_7^-$ as can be expected from the geometry of $Fe_2Cl_7^-$ shown in Fig. 2. The Cl 2p spectra of $[BMIm]FeCl_4$ and $[BMIm]Fe_2Cl_7$ after being reduced by DEAC also exhibited two peaks at 199.8 and 198.6 eV for $[BMIm]FeCl_4$ and 200.7 and 199.0 eV for $[BMIm]Fe_2Cl_7$ with the area ratios of 1:1.3 and 1:5.7, respectively. The binding energy of Cl will be smaller for Fe(II) than that for Fe(III), and therefore the higher Cl content in the lower binding energy state for $[BMIm]Fe_2Cl_7$ species implies that $[BMIm]Fe_2Cl_7$ is more susceptible to the reduction by DEAC than $[BMIm]FeCl_4$.

As shown in Fig. 4, the catalytic system producing higher yields of H_{nn} showed higher contents of Fe(II) and Fe(0) species. The amount of reduced Fe species at the same molar ratio of DEAC/Fe(III) was larger for $[BMIm]Fe_2Cl_7$ than for $[BMIm]FeCl_4$. It is not clear at the moment which reduced species, Fe(II) or Fe(0), is responsible for the formation of H_{nn}, but Fe(II) species seems to be more in charge of the formation of H_{nn}. This is somewhat supported by the separate experiments with $FeCl_2$ and Fe(0). As seen in Table 3, the dimerization did not proceed at all when Fe powder, Fe nanoparticles, or $Fe(CO)_5$ was used as the catalyst, irrespective of the presence of [BMIm]Cl and/or DEAC. The reaction was also performed with Fe(0) in the presence of TPP because Fe(0) species such as [Fe(TPP)] and $[Fe(TPP)_2]$ were proposed as active species for the NBD dimerization in the presence of a catalytic system composed of $Fe(acac)_3$, TPP, and DEAC [30]. However, the presence of TPP did not affect the dimerization with Fe(0), clearly showing that active Fe(0) species is not generated from Fe powder, Fe nanoparticles, or $Fe(CO)_5$.

On the contrary, $FeCl_2$ exhibited high NBD conversion and H_{nn} yield, but only in the co-presence of both [BMIm]Cl and DEAC. These results indicate that Fe(II) is an active species and both [BMIm]Cl and DEAC are playing pivotal roles in the activation of $FeCl_2$. The yield of H_{nn} increased with increasing molar ratio of $[BMIm]Cl/FeCl_2$ up to 2 and then remained almost unchanged on further increase of the molar ratio, implying that $[BMIm]_2FeCl_4$ is the precursor to an active species. The behavior of $[BMIm]Cl–FeCl_2$ system is in contrast with that of $[BMIm]Cl–FeCl_3$, with which the yield of H_{nn} decreased with increasing content of [BMIm]Cl, again demonstrating the importance of Fe(II) species. Like in the case of $FeCl_3$, the Fe–Cl bond of $FeCl_2$ becomes lengthened by the interaction with [BMIm]Cl through the formation of $[BMIm]_2FeCl_4$ [31,32], thereby facilitating the interaction with DEAC to generate active species. Since the catalytic system consisting of $FeCl_2$, [BMIm]Cl, and DEAC is active and metallic Fe(0) is inactive for the dimerization, the complete reduction of $FeCl_2$ by DEAC to inactive metallic Fe(0) is highly unlikely. In this regard, the major role of DEAC in the $FeCl_2$-based catalytic system is believed to be the activation of in situ formed $[BMIm]_2FeCl_4$ rather than the reduction of Fe(II) to Fe(0). As an active Fe(II) species, $[Fe(II)Cl]^+$ was considered as the most plausible active species on the basis of theoretical calculation. Moreover, $[Fe(II)Cl]^+$ can easily accommodate two NBD molecules to form $[Fe(II)Cl(NBD)_2]^+$, an intermediate to H_{nn} (see Fig. 6c).

As an active Fe(0) species, Fe(0) with a Cl^- ligand, $[Fe(0)Cl]^-$ could be regarded as a plausible active Fe(0) species because there is no neutral ligand like TPP to stabilize Fe(0) species in our catalytic system. Even though any decisive evidence for the generation $[Fe(0)Cl]^-$ has not been observed, there is a possibility that $[Fe(0)Cl]^-$ could function as an active species because it can bind two NBD molecules to form a stable 18-electron species. However, the possibility of $[Fe(0)Cl]^-$ to act as an active species was excluded based on the theoretical calculation. Nevertheless, the involvement of other type of Fe(0) species such as [Fe(NBD)] and $[Fe(NBD)_2]$ cannot be ruled out even though the stabilization of Fe(0) by NBD would be much weaker than that by TPP [30].

It is noteworthy that the activity of an Fe-containing ionic liquids is not significantly affected by the presence of TPP (Table 2, entry 10), demonstrating that Fe-containing ionic liquid does not generate Fe(0) species like [Fe(TPP)] or $[Fe(TPP)_2]$, which are proposed as active species for the dimerization of NBD in the presence of a catalytic system consisting of $Fe(acac)_3$, TPP, and DEAC [30]. For comparison, NBD dimerization was also conducted at 85 °C with the catalytic system consisting of $Fe(acac)_3$, TPP, and DEAC. The NBD conversion and H_{nn} yield were little lower than those obtained from either $FeCl_2$–[BMIm]Cl–DEAC (1:2:5) or $[BMIm]Fe_2Cl_7$–DEAC (1:5), suggesting that Fe-containing ionic liquid-based catalytic systems are somewhat superior to that based on $Fe(acac)_3$ (see Tables 2 and 3).

From the experimental results, the formation of active species from $[BMIm]Fe_2Cl_7$, $[BMIm]FeCl_4$, and $[BMIm]_2FeCl_4$ by the interaction with DEAC are postulated and depicted in Scheme 2. The reduction of $[BMIm]Fe_2Cl_7$ would proceed through ethyl transfer from DEAC and subsequent reductive elimination of *n*-butane (or ethyl chloride) to generate reduced $([BMIm]Fe_2Cl_5)^*$ and $EtAlCl_2$. Theoretical calculation shows that dimeric structure of $([BMIm]Fe_2Cl_5)^*$ is hard to exist and thus it is assumed that $([BMIm]Fe_2Cl_5)^*$ rapidly transforms into an active Fe(II) species, $[(BMIm)^+(Fe(II)Cl)^+][Fe(II)Cl_4]^{2-}$ as soon as it forms. Since the dimerization reaction proceeds only in the presence of [BMIm]Cl, the involvement of $[BMIm]^+$ moiety in the active species can be rationalized to a certain extent. Alternatively, $([BMIm]Fe_2Cl_5)^*$ can be further reduced to metallic Fe(0) by interacting with DEAC. In fact, metallic Fe(0) precipitates was observed during the dimerization with $[BMIm]Fe_2Cl_7$.

Similarly to $[BMIm]Fe_2Cl_7$, $[BMIm]FeCl_4$ can be reduced by DEAC to give $([BMIm]FeCl_3)^*$, which can be transformed into $[Fe(II)Cl]^+[(BMIm)Cl_2]^-$ or further reduced to Fe(0) (see Eqs. (1)–(5)).

$$2[BMIm]FeCl_4 + 2DEAC \rightarrow 2([BMIm]FeCl_3)^* + 2EtAlCl_2 + n\text{-}C_4H_{10}, \quad (1)$$

$$2([BMIm]FeCl_3)^* \rightarrow 2[Fe(II)Cl]^+[(BMIm)Cl_2]^-, \quad (2)$$

$$([BMIm]FeCl_3)^* + DEAC \rightarrow Fe(0) + [BMIm]Cl + EtAlCl_2 + C_2H_5Cl, \quad (3)$$

$$2([BMIm]FeCl_3)^* + 2DEAC \rightarrow Fe(0) + [BMIm]Cl + 2EtAlCl_2 + n\text{-}C_4H_{10}, \quad (4)$$

$$[BMIm]Cl + EtAlCl_2 \rightarrow [BMIm]EtAlCl_3. \quad (5)$$

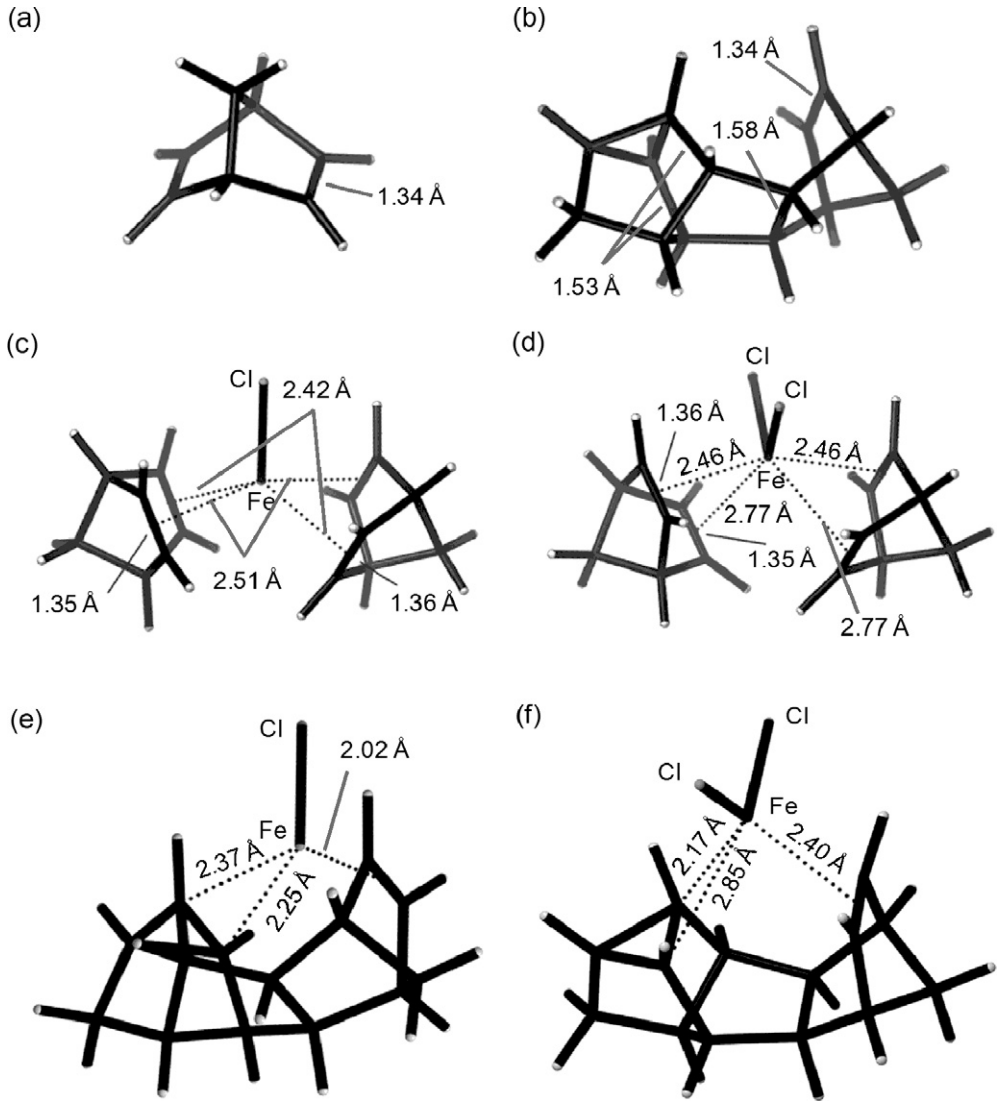

Fig. 6. Optimized structures of: (a) NBD, **1**; (b) H_{nn}, **2**; (c) $[Fe(II)Cl(NBD)_2]^+$, **3a**; (d) $[Fe(III)Cl_2(NBD)_2]^+$, **3b**; (e) $[Fe(II)Cl(H_{nn})]^+$, **4a**; (f) $[Fe(III)Cl_2(H_{nn})]^+$, **4b**.

Unlike the cases of $[BMIm]Fe_2Cl_7$ and $[BMIm]FeCl_4$, the activation of $[BMIm]_2FeCl_4$, formed from the interaction of $FeCl_2$ with two equivalents of [BMIm]Cl, seems to proceed in a different way. The evolution of *n*-butane or ethyl chloride was not observed at temperatures lower than 60 °C upon interaction with DEAC, suggesting that the reduction of $[BMIm]_2FeCl_4$ is much more difficult compared with those of $[BMIm]Fe_2Cl_7$ and $[BMIm]FeCl_4$. Even at 85 °C, only a small amount of *n*-butane was produced. From this result, it is likely that the activation proceeds through the abstraction of Cl^- from $[BMIm]_2FeCl_4$ by DEAC to form $([BMIm]FeCl_3)^*$ and $[BMIm]Et_2AlCl_2$. Even though the reduction of $[BMIm]_2FeCl_4$ by DEAC is hard to take place, there still is a possibility that small portion of $[BMIm]_2FeCl_4$ is reduced to Fe(0) along with the formation of *n*-butane and $[BMIm]EtAlCl_3$ (Scheme 2).

To support our postulate that cationic Fe(II) species is an active species in the dimerization of NBD, the interactions of $[Fe(II)Cl]^+$ and $[Fe(III)Cl_2]^+$ with NBD were theoretically investigated at the B3LYP (6-31+G* for C and H, and LanL2DZ with ECP for Cl and Fe) level of the theory using Gaussian 03 program [20]. Compounds **1**, **2**, **3a**, and **4a** in Fig. 6 are the optimized structures of NBD, H_{nn}, $[Fe(II)Cl(NBD)_2]^+$, and $[Fe(II)Cl(H_{nn})]^+$, respectively. For comparison, optimized structures of $[Fe(III)Cl_2(NBD)_2]^+$ (**3b**) and $[Fe(III)Cl_2(H_{nn})]^+$ (**4b**) were also obtained. Calculation of free energy of formation shows that **3a** is more stable than **3b** by about 7.9 kcal mol^{-1}, suggesting that coordination of NBD to $[Fe(II)Cl]^+$ is more feasible than that to $[Fe(III)Cl_2]^+$ (see supplementary material).

Catalytic cycle for the formation of H_{nn} from two molecules of NBD by $[Fe(II)Cl]^+$ was theoretically investigated. The optimized structures of reaction intermediates and transition states were depicted in Fig. 7, which shows the order of stepwise formation of three σ bonds by breaking three π bonds (see supplementary material for further information on the structures). Reaction profile of the dimerization reaction of NBD by $[Fe(II)Cl]^+$ shown in Fig. 8 indicates that the rate determining step is the formation of the first σ bond connecting two NBD molecules with the activation energy of 35.8 kcal mol^{-1}. As a whole, the reaction is exergornic by 13.1 kcal mol^{-1}. For comparison, the potential energies for the formation of intermediates from the $[Fe(III)Cl_2]^+$-assisted NBD dimerization were also calculated (see supplementary material).

3.4. Effect of molar ratio of NBD/Fe(III)

The effect of NBD/Fe(III) molar ratio on the dimerization of NBD was also investigated. The reactions were conducted at 85 °C and at the DEAC/Fe(III) molar ratio of 5 in the presence of a catalytic system consisting of DEAC and $[BMIm]FeCl_4$ or $[BMIm]Fe_2Cl_7$. As shown in Fig. 9, the conversion of NBD decreased with increas-

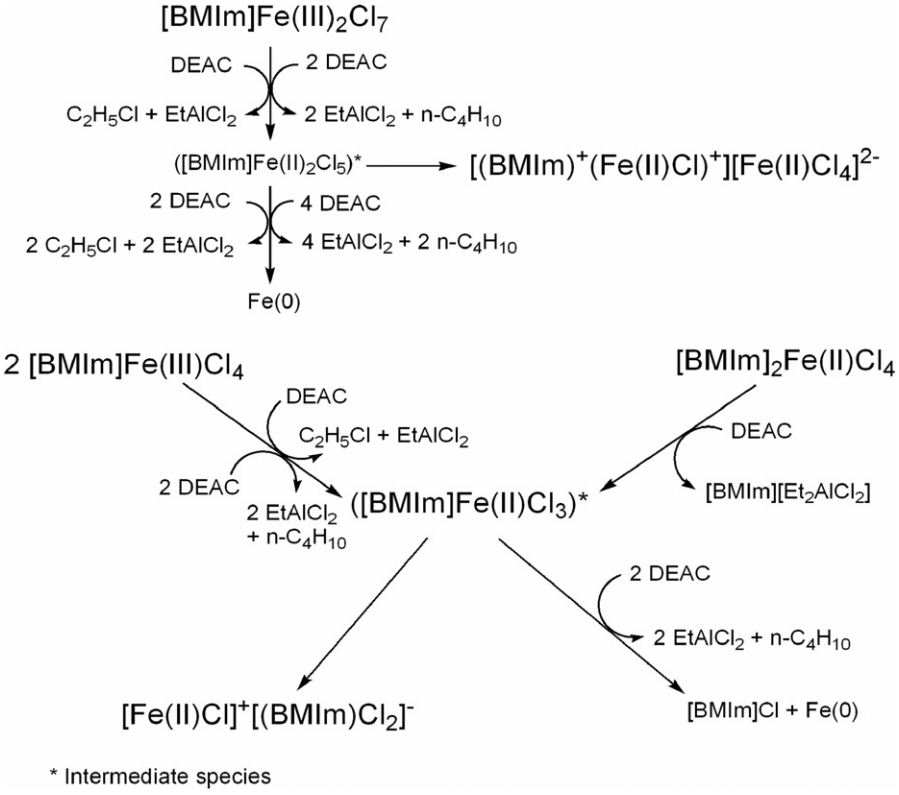

Scheme 2. Plausible mechanisms for the active species, $[Fe(II)Cl]^+$.

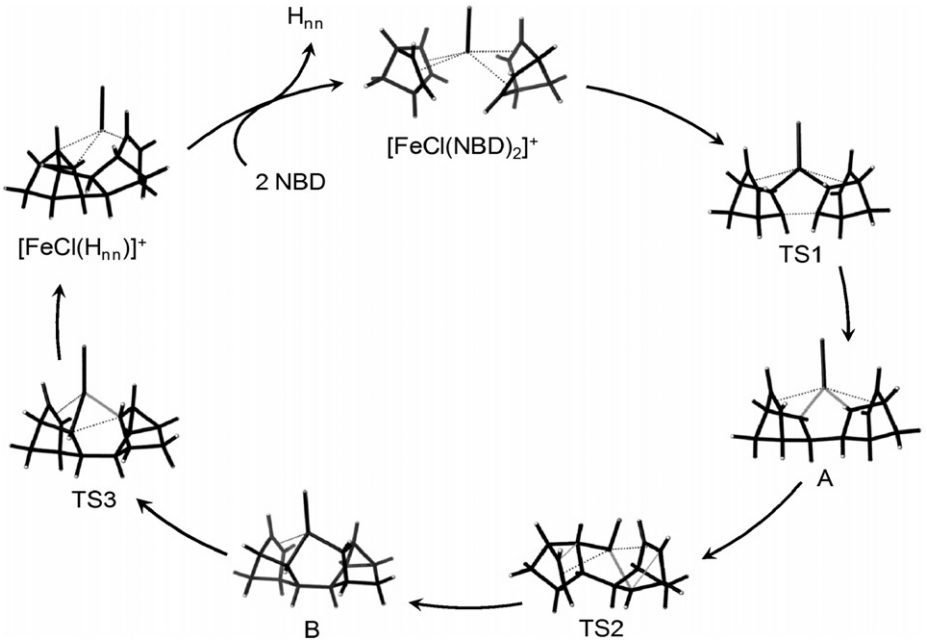

Fig. 7. The optimized structures of reaction intermediates and transition states of dimerization of NBD using $[Fe(II)Cl]^+$ as an active species (TS = transition state; A and B = reaction intermediates).

ing molar ratio of NBD/Fe(III), but the selectivity of H_{nn} increased slowly with the increase of the molar ratio up to 100.

3.5. Effect of temperature

The dimerization reactions of NBD were carried out at various temperatures using a catalytic system consisting of DEAC and [BMIm]$FeCl_4$ or [BMIm]Fe_2Cl_7. As shown in Table 4, the conversion of NBD increased with the temperature rose when the dimerization reactions were conducted with the molar ratio of NBD/Fe(III) at 100. The yield of H_{nn}, however, increased with the increase of temperature only up to 85 °C, and then decreased on further increase of temperature, most likely due to the acceleration of NBD polymerization and to the decomposition of the active species. Larger amounts of metallic particles were observed at 100 °C than at 85 °C.

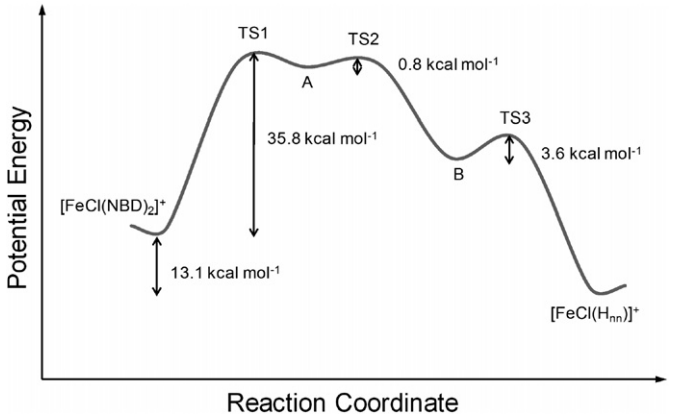

Fig. 8. Reaction profile of the dimerization reaction of NBD by $[Fe(II)Cl]^+$.

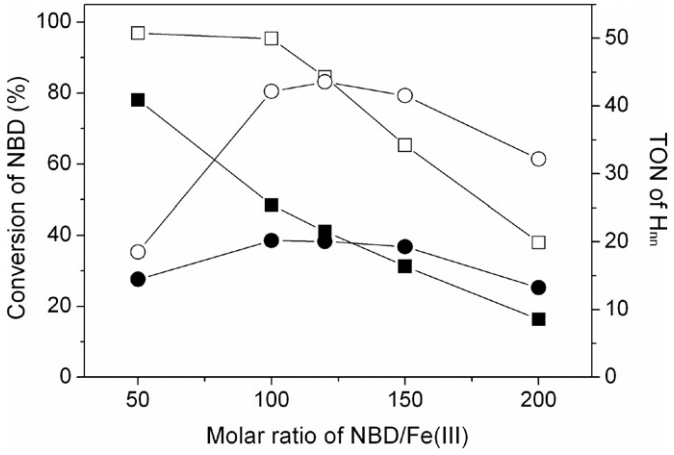

Fig. 9. Effect of the molar ratio of NBD/Fe(III) on the dimerization reaction of NBD: (□) conversion of NBD with $[BMIm]Fe_2Cl_7$; (■) conversion of NBD with $[BMIm]FeCl_4$; (○) TON of H_{nn} with $[BMIm]Fe_2Cl_7$; (●) TON of H_{nn} with $[BMIm]FeCl_4$ (TON = mol of H_{nn}/mol of Fe(III), reaction condition: molar ratio of DEAC/Fe(III) = 5, temperature = 85 °C, reaction time = 1 h).

Table 4
Effect of temperature on the dimerization reaction of NBD[a]

Entry	Catalyst	Temperature (°C)	C[b] (%)	S[c] (%)	Y[d] (%)
1	$[BMIm]FeCl_4$	25	1.7	57	1
2	$[BMIm]FeCl_4$	40	5.3	69.5	3.7
3	$[BMIm]FeCl_4$	60	40.1	78.8	31.6
4	$[BMIm]FeCl_4$	85	48.5	83.2	40.4
5	$[BMIm]FeCl_4$	100	63.1	57.3	36.2
6	$[BMIm]Fe_2Cl_7$	25	3.4	68.9	2.3
7	$[BMIm]Fe_2Cl_7$	40	8.2	74.6	6.1
8	$[BMIm]Fe_2Cl_7$	60	85.2	82	69.9
9	$[BMIm]Fe_2Cl_7$	85	95.4	88.4	84.3
10	$[BMIm]Fe_2Cl_7$	100	97.4	78.7	76.7

[a] Molar ratio of NBD/Fe(III) = 100/1, DEAC/catalyst = 5, temperature = 85 °C, reaction time = 1 h.
[b] Conversion of NBD.
[c] Selectivity of H_{nn}.
[d] Yield of H_{nn}.

3.6. Effect of reaction time

Effect of reaction time was also examined using $[BMIm]FeCl_4$ and $[BMIm]Fe_2Cl_7$ at 85 °C. The molar ratios of NBD/Fe(III) and DEAC/Fe(III) were set at 100 and 5, respectively. As shown in Fig. 10, the conversion of NBD increased rapidly with the reaction time, but the rate of increase was much slower after 30 min for both catalysts. It seems that the system reaches a maximum of conversion in less than an hour.

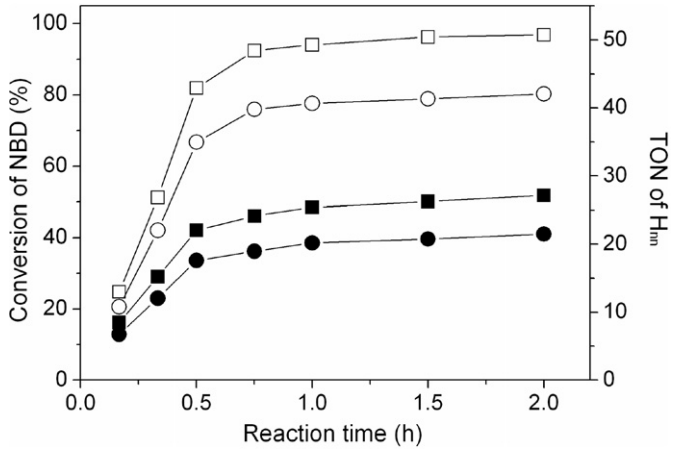

Fig. 10. Effect of reaction time on the dimerization reaction of NBD at 85 °C: (□) conversion of NBD with $[BMIm]Fe_2Cl_7$; (■) conversion of NBD with $[BMIm]FeCl_4$; (○) TON of H_{nn} with $[BMIm]Fe_2Cl_7$; (●) TON of H_{nn} with $[BMIm]FeCl_4$; (TON = mol of H_{nn}/mol of Fe(III), molar ratios of NBD/Fe(III) and DEAC/Fe(III) were set at 100 and 5, respectively).

Table 5
Catalyst recycling study with $[BMIm]Fe_2Cl_7$[a]

Cycle No.	Conversion of NBD (%)	Selectivity of H_{nn} (%)	Yield of H_{nn} (%)
1	94.1	86.4	81.3
2	88.3	85.9	75.8
3	66	87.7	57.9
4	48.7	86.2	42.0

[a] Molar ratio of NBD/Fe(III) = 100/1, DEAC/catalyst = 5, temperature = 85 °C, reaction time = 1 h.

3.7. Catalyst recycling

To test the catalyst stability and recyclability, the dimerization reaction of NBD was performed with $[BMIm]Fe_2Cl_7$ for 1 h at 85 °C at the ratios of NBD/Fe(III) = 100/1, DEAC/catalyst = 5, respectively. After the reaction, most of volatile compounds were removed under a reduced pressure and the remaining catalyst mixture was reused for further reactions with fresh charges of NBD and toluene. As seen in Table 5, both NBD conversion and H_{nn} yield were found to decrease continuously with the recycles. This can be largely attributed to the reduction of Fe(II) to inactive Fe(0) and to the accumulation of high boiling side products.

4. Conclusion

Fe-containing IL catalysts, $[BMIm]FeCl_4$, $[BMIm]Fe_2Cl_7$, and $[BMIm]_2FeCl_4$ were highly effective for the selective dimerization of NBD to produce H_{nn} in high yield. By employing these catalysts, the use of expensive phosphanes was avoided and the required amount of reducing agent (DEAC) was greatly reduced. From the mechanistic and theoretical studies on the active species, experimental results on the dimerization, and Tafel measurements, it is postulated that the active species, $[Fe(II)Cl]^+$, is in charge of the H_{nn} formation. The roles of [BMIm]Cl are believed to promote the generation of the active species through the formation of easily reducible $[BMIm]Fe_xCl_{3x+1}$ ($x = 1$ or 2) or $[BMIm]_2FeCl_4$, and to stabilize the resulting active species.

Further study is in progress to improve the catalyst stability and recyclability using polymer-supported catalysts for the practical application.

Acknowledgment

We acknowledge financial support by a grant (CF2-101-1) from Carbon Dioxide Reduction & Sequestration Research Center, one of the 21st Century Frontier Programs funded by the Ministry of Science and Technology of Korean government.

Supplementary material

The online version of this article contains additional supplementary material.

Please visit DOI: 10.1016/j.jcat.2008.05.008.

References

[1] H.K. Myers Jr., A. Schneider, US Patent 4208355 (1980).
[2] J.M. Burlitch, S.E. Hayes, J.T. Lemley, Organometallics 4 (1985) 167.
[3] M. Lautens, W. Tam, C. Sood, J. Org. Chem. 58 (1993) 4513.
[4] J. Blum, F. Gelman, R. Abu-Reziq, I. Miloslavski, H. Schumann, D. Avnir, Polyhedron 19 (2000) 509.
[5] J.R. Thomas, US Patent 4094916 (1978).
[6] J.R. Thomas, US Patent 4094917 (1978).
[7] G. Suld, A. Schneider, H.K. Myers Jr., US Patent 4207080 (1980).
[8] V.R. Flid, O.S. Manulik, A.A. Grigor'ev, A.P. Belov, Kinet. Catal. 39 (1998) 51.
[9] D.-J. Huang, C.-H. Cheng, J. Organomet. Chem. 490 (1995) C1.
[10] V.R. Flid, V.B. Kuznetsov, A.A. Grigor'ev, A.P. Belov, Kinet. Catal. 41 (2000) 604.
[11] V.R. Flid, O.S. Manulik, A.A. Grigor'ev, A.P. Belov, Kinet. Catal. 41 (2000) 597.
[12] A. Schneider, H.K. Myers Jr., G. Suld, US Patent 4275254 (1981).
[13] H. Brunner, F. Prester, Tetrahedron: Asymm. 1 (1990) 589.
[14] S. Tanaka, C. Dubs, A. Inagaki, M. Akita, Organometallics 24 (2005) 163.
[15] S.K. Brayshaw, J.C. Green, G. Kociok-Kohn, E.L. Sceats, A.S. Weller, Angew. Chem. Int. Ed. 45 (2006) 452.
[16] T. Ooi, J. Morikawa, D. Uraguchi, K. Maruoka, Tetrahedron Lett. 40 (1999) 2993.
[17] P. Wasserscheid, J. Ind. Eng. Chem. 13 (2007) 325.
[18] W.L.F. Armarego, C.L.L. Chai, in: Purification of Laboratory Chemicals, fifth ed., Elsevier, 2003, p. 370.
[19] V. Farmer, T. Welton, Green Chem. 4 (2002) 97.
[20] M. Sitze, E.R. Schreiter, E.V. Patterson, R.G. Freeman, Inorg. Chem. 40 (2001) 2298.
[21] Y. Yoshida, G. Saito, J. Mater. Chem. 16 (2006) 1254.
[22] Y.J. Kim, C.R. Park, Inorg. Chem. 41 (2002) 6211.
[23] J.F. Moulder, W.F. Stickle, P.E. Sobol, K.D. Bomben, in: J. Chanstain, R.C. King Jr. (Eds.), Handbook of X-Ray Photoelectron Spectroscopy—A Reference Book of Standard Spectra for Identification and Interpretation of XPS Data, Physical Electronics Inc., Eden Prairie, MN, 1995.
[24] G. Johansson, J. Hedman, A. Berndtsson, M. Dlasson, R. Nilsson, J. Electron Spectrosc. Relat. Phenom. 2 (1973) 295.
[25] N. Acton, R.J. Roth, T.J. Katz, J.K. Frank, C.A. Maier, I.C. Paul, J. Am. Chem. Soc. 94 (1972) 5446.
[26] K.M. Dieter, C.J. Dymek Jr., N.E. Heimer, J.W. Rovang, J.S. Wilkes, J. Am. Chem. Soc. 110 (1988) 2722.
[27] C.L. Hussey, Pure Appl. Chem. 60 (1988) 1763.
[28] S. Zhang, Q. Zhang, Z.C. Zhang, Ind. Eng. Chem. Res. 43 (2004) 614.
[29] P.C.J. Graat, M.A.J. Somers, Appl. Surf. Sci. 100/101 (1996) 36.
[30] S.M. Pillai, G.L. Tembe, V.J. Koshy, M. Ravindranathan, P.S. Venkataramani, S.L. Kalra, R. Singh, H.C. Srivatsava, R. Tiwari, O. Prakash, New J. Chem. 20 (1996) 677.
[31] M.S. Sitze, E.R. Schreiter, E.V. Patterson, R.G. Freeman, Inorg. Chem. 40 (2001) 2298.
[32] D. Yin, C. Li, L. Tao, N. Yu, S. Hu, D. Yin, J. Mol. Catal. A Chem. 245 (2006) 260.